

Assimilation in the upper-troposphere and lower-stratosphere: The role of GPS radio occultation

Sean Healy

*ECMWF, Shinfield Park, Reading
RG2 9AX, United Kingdom
sean.healy@ecmwf.int*

ABSTRACT

GPS radio occultation (GPS-RO) measurements are now assimilated routinely at most operational numerical weather prediction centres. The measurements have a large impact on upper-tropospheric and lower-stratospheric temperatures. They complement information provided by satellite radiances because they have good vertical resolution, and they can be assimilated without bias correction. This paper describes the GPS-RO measurement technique, and outlines the main pre-processing steps required to produce both the assimilated quantities and the retrieved geophysical variables, from the “raw” measurements of a time-delay. The GPS-RO temperature “null-space” is explained, and it is shown that some stratospheric temperature biases are difficult to detect and correct. Some results from recent forecast impact experiments are presented showing that GPS-RO has a positive impact from day-1 to day-7 on stratospheric geopotential heights in the Southern Hemisphere. Time-series from the ERA-Interim reanalysis are used to show the consistency of the bending angle departure statistics from different GPS-RO missions. The possible use of GPS-RO for forecast verification in the stratosphere is noted.

1 Introduction

The radio occultation measurement technique was pioneered by the planetary science community in the 1960’s, and formed part of NASA’s Mariner 3 and 4 missions to Mars (See Yunck *et al.*, (2000) for a history of GPS sounding). The measurement is based on simple physics, observing how the paths of radio waves propagating through an atmosphere are refracted or “bent” as a result of refractive index gradients. The original radio occultation concept envisaged by the planetary scientists was a fleeting, fly-by encounter, as a spacecraft passed behind a planet, but it was noted as early as 1965 that the method could be adapted to measure the Earth’s atmosphere. However, the required infrastructure – a constellation of radio transmitters orbiting the Earth – was considered un-affordable at that time.

In the late 1980’s it was recognised that the GPS satellites, which are primarily designed as a tool for precise positioning and navigation, would be a suitable source of radio signals, and the concept of GPS radio occultation (GPS-RO) began to be explored. In 1995, work at the University Corporation for Atmospheric Research (UCAR) and the Jet Propulsion Laboratory (JPL) culminated in the launch of the “proof of concept” GPS/MET instrument into a low earth orbit (LEO). This mission placed a GPS receiver developed at JPL in space, and enabled the first GPS-RO measurements to be made. Figure 1 shows the geometry of the GPS-RO measurement technique. The radio signal is transmitted by a GPS satellite, passes through the neutral atmosphere and ionosphere and is measured with a GPS receiver placed on a LEO satellite. Kursinski *et al.* (1996) and Rocken *et al.* (1997) demonstrated that GPS-RO temperature retrievals agreed with radiosondes and numerical weather prediction (NWP) analyses to within ~ 1 K, in the vertical interval between 7 km to 25 km, essentially using a retrieval technique developed by the planetary scientists. The success of GPS-MET led to a number of missions of opportunity, such as CHAMP (Wickert *et al.*, 2001), the COSMIC constellation of six satellites (Anthes *et al.*, 2008), and the GRAS GPS-RO instrument on the Metop satellites (Luntama *et al.*, 2008).

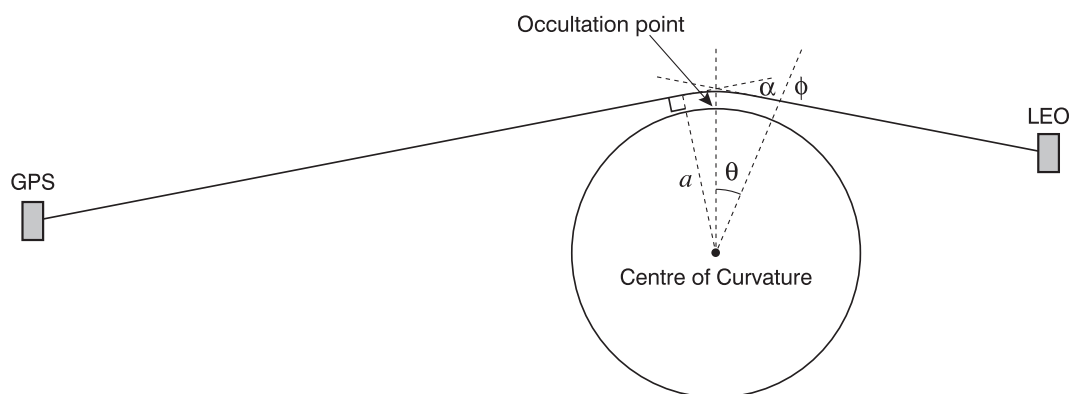


Figure 1: The geometry of the GPS-RO measurement technique. The GPS signals propagate through the ionosphere and neutral atmosphere, and the path is bent by refractive index gradients. The ray bending is characterised by angle α , as a function of impact parameter, a . The bending angles for tangent heights near the surface are typically 1-2 degrees. The bending falls exponentially with tangent point height.

The potential use of GPS-RO in NWP using variational retrieval/assimilation techniques was first discussed by Eyre (1994). New data types are only really valuable in NWP if they provide information that is not already provided by other parts of the global observing system, and the availability of GPS-RO coincided with a significant increase in the number of satellite radiances assimilated from advanced sounders such as AIRS. Nevertheless, in recent years most operational NWP centres have reported a positive forecast impact as a result of assimilating GPS-RO data, with the largest signal on the upper-tropospheric and lower/middle-stratospheric temperatures (e.g., Healy, 2008; Cucurull *et al.*, 2007; Aparicio and Deblonde, 2008; Poli *et al.*, 2009; Rennie, 2010). This is also confirmed in the most recent set of observing system experiments using the ECMWF system, which are presented by McNally in this volume.

The GPS-RO measurements have a clear impact and role in NWP systems because they complement the information provided by satellite radiances. This is because 1) they have good vertical resolution and 2) they can be assimilated without bias correction, meaning they are “anchor measurements”, so they can constrain the bias corrections applied to radiances.

This paper describes the GPS-RO measurement technique, briefly summarises the current impact in NWP systems and the climate monitoring applications. The retrieval approach developed by the planetary science community is outlined in section 2. The assimilation of GPS-RO measurements into NWP systems is described in section 3, including the forward models, the assumed error statistic models and the GPS-RO null-space. A summary of the impact of GPS-RO in NWP and climate applications is presented in section 4. The discussion and concluding remarks are given in section 5.

2 A GPS-RO retrieval scheme

The geophysical retrieval approach developed by the planetary scientists provides a convenient framework for understanding the GPS-RO measurement technique. A number of authors provide a more detailed description of the basic physics and processing of the GPS-RO measurements (see e.g., Kursinski *et al.*, 1997; Hajj *et al.*, 2002).

The measurement geometry is illustrated in Figure 1, and for simplicity we will consider single path propagation, where only one ray-path links the satellites at any given time. Complications arising from

“multipath” propagation, where multiple rays arrive at the receiver at the same time, are important in the lower-troposphere. These can be mitigated with more complex wave optics processing techniques (e.g., Gorbunov and Lauritsen, 2004), but they will not be discussed here.

GPS-RO is not a direct measurement of temperature. The temperature information is produced with a geophysical retrieval, which requires *a priori* information and assumptions to obtain the geophysical variables. The fundamental – or raw – measurement of the GPS-RO technique is the time required for a radio signal to propagate from a GPS satellite to a receiver on board a low earth orbiting (LEO) satellite, which is measured with an atomic clock. The neutral atmosphere and ionosphere modify the speed of the signal because the refractive index along the path is not unity, and the ray-path between the satellites is curved as a result of gradients in the refractive index. These effects combine to produce an excess phase delay, relative to that expected for a straight line path between the satellites in a vacuum.

The current GPS satellites transmit L band signals at frequency $f_{L1}=1575.42$ MHz and $f_{L2}=1227.60$ MHz. The motion of the LEO means that vertical profiles of the phase delays at the L1 and L2 frequencies can be determined. The L1 and L2 phase delays are “calibrated” to account for special and general relativistic effects, and to remove clock errors (Hajj *et al.*, 2002). The two time-series of calibrated excess phase delays are then differentiated with respect to time to provide time-series of L1 and L2 Doppler shifts. Note that the Doppler shift values are not sensitive to fixed biases in the excess phase measurements as a result of the differentiation.

The Doppler shift is related to the bending along the ray-path, which is characterised by the bending angle α_i , where the subscript is $i = 1, 2$, for the L1 and L2 signals, respectively. However, deriving α_i from the Doppler shift is an ill-posed problem. It is made well-posed by *assuming* that the variable known as the impact parameter, a , has the same value at the GPS and LEO satellites. This enables α_i and a to be derived simultaneously, given accurate estimates of satellite position and velocities, and assuming the refractive index is unity at the satellites.

At this stage the bending angle contains contributions from the neutral atmosphere and the ionosphere. Fortunately, the ionosphere is dispersive and the ionospheric bending can be removed – or corrected – to first order by taking a linear combination of the L1 and L2 bending angle values (Vorob’ev and Krasil’nikova, 1994). The corrected bending angle, $\alpha(a)$, is given by,

$$\alpha(a) = \alpha_1(a) + \frac{f_{L2}^2}{f_{L1}^2 - f_{L2}^2} (\alpha_1(a) - \alpha_2(a)) \quad (1)$$

where the L1 and L2 bending angles have been interpolated to a common impact parameter, a . Residual ionospheric noise is one of the factors limiting the information content of corrected bending angles above $\sim 35 - 40$ km. There is also a concern that this ionospheric correction method produces biases that vary during the solar cycle (Danzer *et al.*, 2013) and this may affect climate monitoring applications. This is an area of active research.

To first order, the ionospheric corrected bending angle falls exponentially with height, with a scale height equal to the density scale height. The horizontal weighting function $d\alpha/ds$ is a Gaussian centred on the assumed tangent point. The width of Gaussian scales as $w \sim \sqrt{r_e H}$, where r_e is the radius of the Earth and H is the scale height. Hence, for an exponentially decaying atmosphere with a scale height of $H \sim 7$ km, around two thirds of the ray bending occurs over a $\sim 2\sqrt{r_e H} \sim 400$ km section of ray-path centred on the tangent point location.

The corrected bending angles are smoothed and extrapolated to infinity in a process known as “statistical optimization”. The statistically optimized bending angles, α_{so} , are a linear combination of the ionospheric corrected bending angles, α , and simulated values produced with a atmospheric climatology, α_b . They can be written in terms of a matrix/vector equation,

$$\alpha_{so} = \alpha_b + \mathbf{K}(\alpha - \alpha_b) \quad (2)$$

where \mathbf{K} is the gain matrix, which is a function of the assumed error covariance matrices for the observed and background/climatological bending angle profiles.

Assuming spherical symmetry, the refractive index, n , can be derived from the profile of statistically optimised bending angles, $\alpha_{so}(a)$, using an Abel transform,

$$n(x) = \exp \left[\frac{1}{\pi} \int_x^\infty \frac{\alpha_{so}(a)}{(a^2 - x^2)^{1/2}} da \right] \quad (3)$$

where $x = nr$ and r is the radius.

In its simplest form the ‘‘refractivity’’, defined as $N = 10^6(n - 1)$, is given by,

$$N = \frac{c_1 P}{T} + \frac{c_2 P_w}{T^2} \quad (4)$$

where P is the total pressure, P_w is the water-vapour pressure, and T is the temperature. The coefficients $c_1 = 77.6\text{K/hPa}$ and $c_2 = 3.73 \times 10^5 \text{K}^2/\text{hPa}$ are derived empirically (Bean and Dutton, 1968). More complex formulations of the refractivity, including both non-ideal gas effects and using improved coefficients have also been proposed (e.g., Aparicio and Laroche 2011).

In the stratosphere $P_w \sim 0$, so the refractivity, N , is linearly proportional to the density, ρ ,

$$\rho = \frac{N}{c_1 R} \quad (5)$$

where R is the ideal gas constant. This means that a profile of N can be vertically integrated to provide pressure as a function of height, using the hydrostatic relationship. A temperature profile can then be derived using the ideal gas law. However, note again that some *a priori* information is required to initialise the hydrostatic integration (see Kursinski *et al.*, 1997).

In the troposphere additional *a priori* is required to retrieve temperature and humidity information from the refractivity profile. Information content studies suggest that the measurements primarily contain water vapour information in the lower-troposphere, although to date this has been difficult to demonstrate conclusively in modern NWP systems.

3 Assimilation of GPS-RO

3.1 Forward Modelling

The assimilation options for GPS-RO are discussed in Eyre (1994). Most operational NWP centres have assimilated either refractivity or ionospheric corrected bending angle profiles, although in recent years there has been gradual move towards assimilating the bending angles (e.g. Rennie 2010; Cucurull *et al.* 2013). One of the advantages of assimilating bending angle rather than refractivity is that it circumvents the statistical optimization processing step. This enables the bending angles to be assimilated to higher altitudes than the refractivity because the latter contains climatology information.

ECMWF currently assimilates ionospheric corrected bending angles with a one-dimensional (1D) operator, but it will move to assimilation with a two-dimensional operator in 2015. These operators are part of the EUMETSAT ROM SAF ROPP software package, and are available from:

<http://www.romsaf.org/software.php>.

The 1D observation operator evaluates the ionospheric corrected bending angle integral, α , as a function of impact parameter, a , by integrating

$$\alpha(a) \simeq -10^{-6} \sqrt{2a} \int_a^\infty \frac{dN}{(x-a)^{1/2}} dx \quad (6)$$

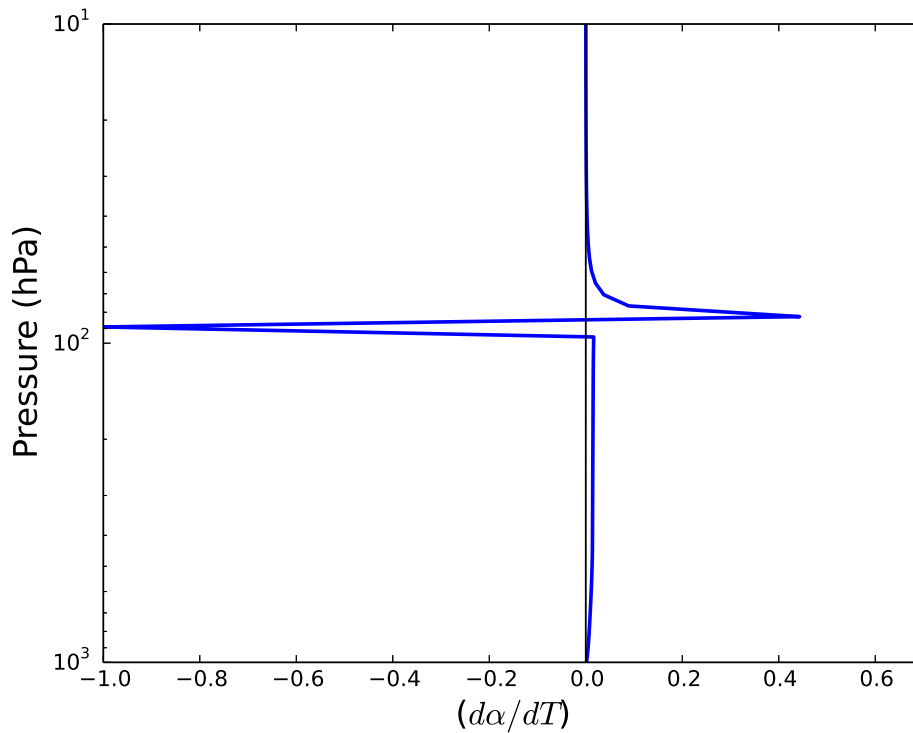


Figure 2: The temperature weighting function, $(\partial\alpha/\partial T)$, for stratospheric bending angle. The largest contributions are from the model levels directly above and below the observed tangent height. The long “hydrostatic” tail below the tangent point is caused by the sensitivity of the stratospheric model level heights to the tropospheric temperatures.

where N , is the refractivity derived from the model and $x = (1 + 10^{-6}N)r$, where r is the radius value of a point on the ray-path. The solution of this integral used at ECMWF is given by Burrows *et al.*, (2014). An alternative approach is presented by Cucurull *et al.*, (2013).

The ROPP operator includes non-ideal gas effects in both the computation of geopotential heights of the model levels and the refractivity values on the model levels (Healy 2011). The drift of the tangent point during an occultation is now included, as originally suggested by Cucurull *et al.*, (2007) and Poli *et al.*, (2009).

We currently use a single combined observation plus forward model error covariance matrix globally for all GPS-RO instruments. The standard deviations of the combined errors are assumed to vary with impact height, h , which is defined as the impact parameter, a , minus the radius of curvature value, R_c , provided with the measurement. The percentage error is assumed to be 20% of the observed value at $h = 0$, falling linearly with h to 1 % at $h = 10$ km. Above 10 km, the error is assumed to be 1% of the observed value until this reaches a lower limit of 3×10^{-6} radians. The errors are assumed to be uncorrelated in the vertical. This is a fairly coarse error model and it should be refined, but it is reasonably consistent with the observed bending angle departure statistics. Other centres, for example the Met Office, employ an error statistic model that varies with latitude (e.g., Rennie, 2010).

3.2 GPS-RO weighting functions and null-space

One of the strengths of GPS-RO, in comparison to radiances from satellite sounders, is superior vertical resolution. Figure 2 shows a temperature weighting function ($\partial\alpha/\partial T$), for a computed bending angle with a tangent point in the lower-stratosphere. The structure of the weighting functions was first described by Eyre (1994). There is a large sensitivity to the temperature at the model level directly above and below the ray tangent height. Noting that the bending angle is related to *minus* the vertical refractivity gradient (Eq.6), increasing the temperature on the model level directly below the tangent point reduces the bending angle (Eq.4), and conversely increasing the temperature on the model level directly above increases the bending angle. Lower down, below 100 hPa in this case, there is a long positive ‘‘hydrostatic tail’’. This is caused by the sensitivity of the computed bending angles to the model level heights. For example, increasing the temperature in the troposphere increases the heights of the model levels in the stratosphere, and this increases the computed stratospheric bending angles. This sensitivity to the model levels heights also means that GPS-RO measurements provide surface pressure information (Healy, 2013).

The sharp GPS-RO weighting functions mean that the measurements can detect and correct small scale forecast errors that are in the ‘‘null-space’’ of satellite radiances, because the radiances are broad vertical averages. The null-space is defined as the set of atmospheric profile perturbations that have negligible impact on the measurement values, when compared with the assumed errors (Rodgers, 2000). It is interesting to note that GPS-RO measurements also have a null-space because they are not a direct measurement of temperature. The GPS-RO null-space arises because the measurements are essentially related to density ($\rho \propto P/T$) as a function of height, and *a priori* information, such as the height of a pressure level, is required to split the combined dependence on pressure and temperature. For example, an exponentially growing temperature error of the form

$$\delta T(z) \propto \exp(-z/H) \quad (7)$$

where z is height, and H is the density scale-height, is difficult to detect with GPS-RO because the density as a function of height remains almost unchanged. Clearly, an exponentially growing temperature error quickly gives rise to totally unphysical geopotential heights of pressure levels, but more subtle biases can be harder to detect. Figure 3 shows a temperature bias that developed over the South Pole in a forecast experiment where radiances were blacklisted but GPS-RO was being assimilated. It was initially surprising that the GPS-RO measurements were unable to detect and correct biases ~ 1 -2 K between 20 - 30 km, which is in the GPS-RO ‘‘core region’’, where the measurement information content is largest. However, when this particular bias profile is propagated through the tangent-linear of the bending angle operator it produces virtually no change in the bending angles between 20 - 30 km. This is illustrated in Figure 4 which shows both the percentage change in computed bending angles, and the assumed standard deviation of the bending angle errors. The GPS-RO measurements cannot constrain this bias because it is in the null-space. Interestingly, we have found that if a sinusoidal temperature perturbation is added to bias shown in Figure 3, this produces a clear sinusoidal bending angle perturbation, but the underlying large-scale bias is not captured. It is also noteworthy that Steiner *et al.*, (Figure 8, 1999) produced a temperature ‘‘retrieval error’’ extremely similar to Figure 3 by perturbing their *a priori* bending angle values used in the statistical optimization by 5 %.

In summary, it should be noted that GPS-RO cannot constrain all model temperature biases in the stratosphere, and it appears that temperature biases that increase gradually with height can be particularly problematic.

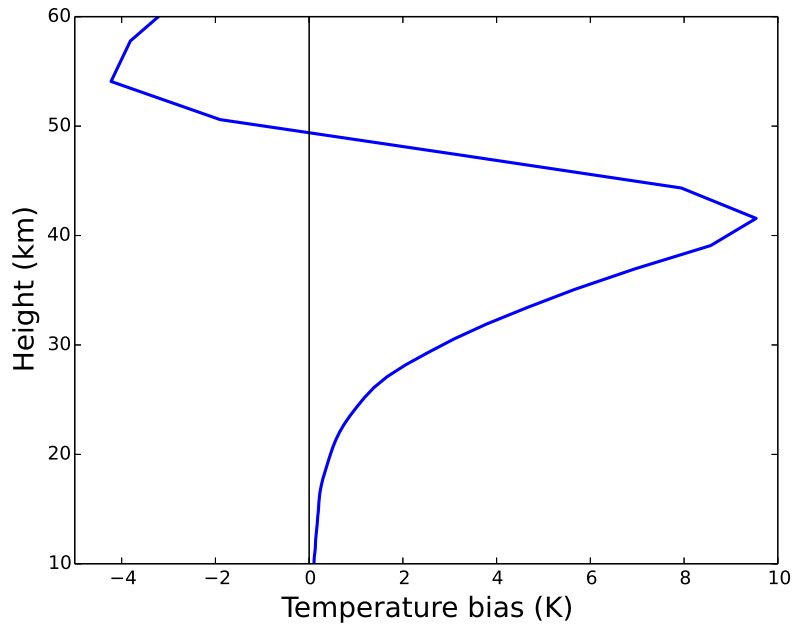


Figure 3: The vertical profile of a temperature bias that developed in Antarctica in a forecast impact experiment where GPS-RO measurements are assimilated. The GPS-RO measurements were unable to correct this bias.

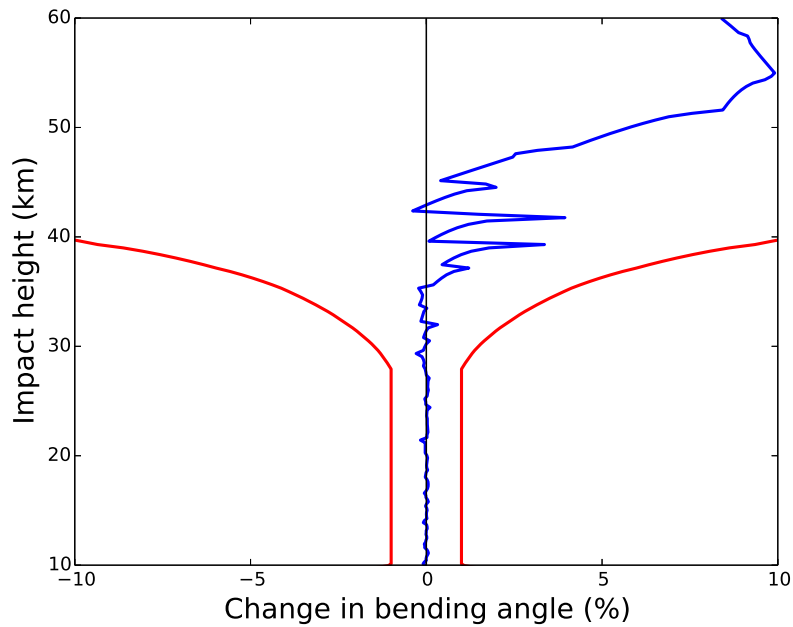


Figure 4: The percentage change in bending angle caused by propagating the temperature bias shown in Figure 3 through the tangent-linear of the bending angle forward model (blue line). The assumed standard deviation of the bending angle errors used when assimilating the data are shown in red for comparison.

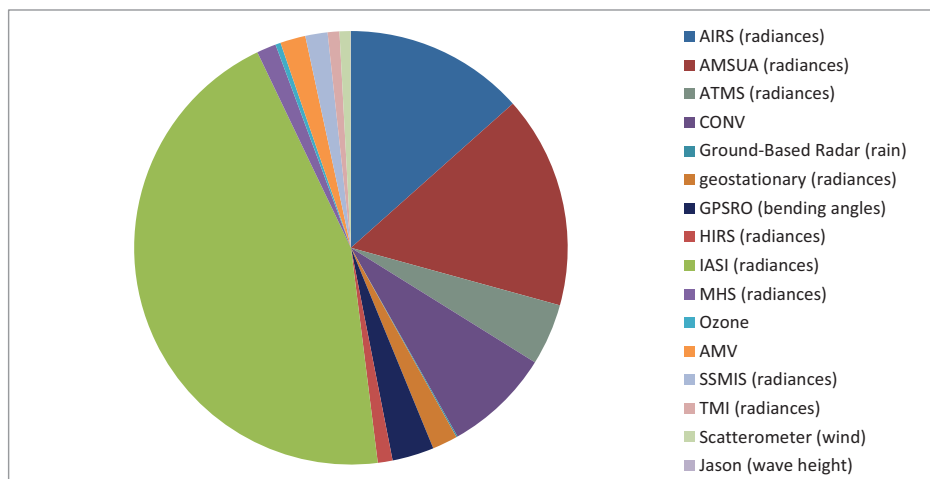


Figure 5: A breakdown of the data assimilated into the ECMWF NWP system for April 2014.

4 Results

4.1 NWP

As noted in the introduction, many operational NWP centres have reported a positive impact as a result of assimilating GPS-RO measurements (e.g., Healy 2008; Cucurull *et al.*, 2007; Aparicio and Deblonde 2008; Poli *et al.*, 2009; Rennie 2010). Cardinali and Healy (2014) have also assessed the impact of GPS-RO on 24 hour forecasts using adjoint-based techniques, and shown that the impact is largest in the lower/middle-stratosphere. The ability of GPS-RO measurements to anchor the bias corrections applied to stratospheric radiances has also been investigated (e.g., Bauer *et al.*, 2014; Cucurull and Anthes, 2014).

GPS-RO bending angles typically represent only $\sim 3\text{-}4\%$ of the total number of observations assimilated into the ECMWF system (Figure 5). The most recent set of observing system experiments with the ECMWF NWP system are reported by McNally in this volume, where both tropospheric and stratospheric scores are examined. The GPS-RO measurements clearly have an impact on tropospheric wind, temperature and humidity scores, but the largest impact is on the stratospheric temperatures. In particular, it is shown that GPS-RO has a larger impact on 100 hPa temperature RMS errors than the other satellite observing systems, and this is largely a result of reducing biases. However, GPS-RO measurements also have a clear impact on the random errors at both the short and medium-range. For example, Figure 6 shows the short-range forecast fit to radiosonde temperature measurements in the Southern Hemisphere. The reduction in the standard deviations are small ($\sim 0.05\text{K}$) but they are statistically significant above 400 hPa. More generally, it is usually the case that assimilating GPS-RO measurements improves the radiosonde temperature departure statistics in the stratosphere, suggesting that these observation types provide consistent information.

Figures 7 and 8 show the fractional reduction of the standard deviation of geopotential height errors at 500, 200, 100 and 50 hPa, verified against radiosonde observations for the Northern and Southern Hemisphere, respectively. As expected, the impacts are larger in the Southern Hemisphere. There is clearly a positive impact at 500 hPa for day-1 and day-2 in both hemispheres, but the impacts are larger, and tend to persist to longer forecast ranges at 100 hPa and 50 hPa. The improvements at 100 hPa and 50 hPa are statistically significant from day-1 to day-7 in the Southern Hemisphere. Similar results are found when verifying against operational NWP analyses.

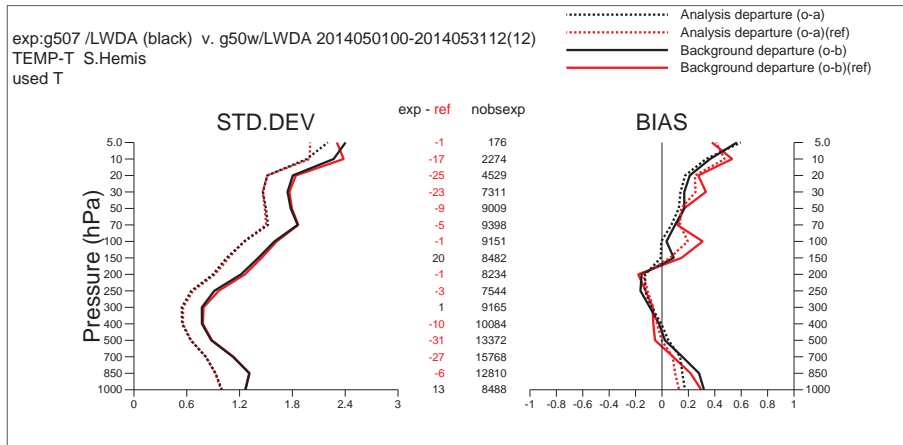


Figure 6: The mean and standard deviation of the (o-b) and (o-a) radiosonde temperature (K) departure statistics in the Southern Hemisphere for May 1-31, 2014. The black lines are when GPS-RO are assimilated and the red lines are when GPS-RO are blacklisted.

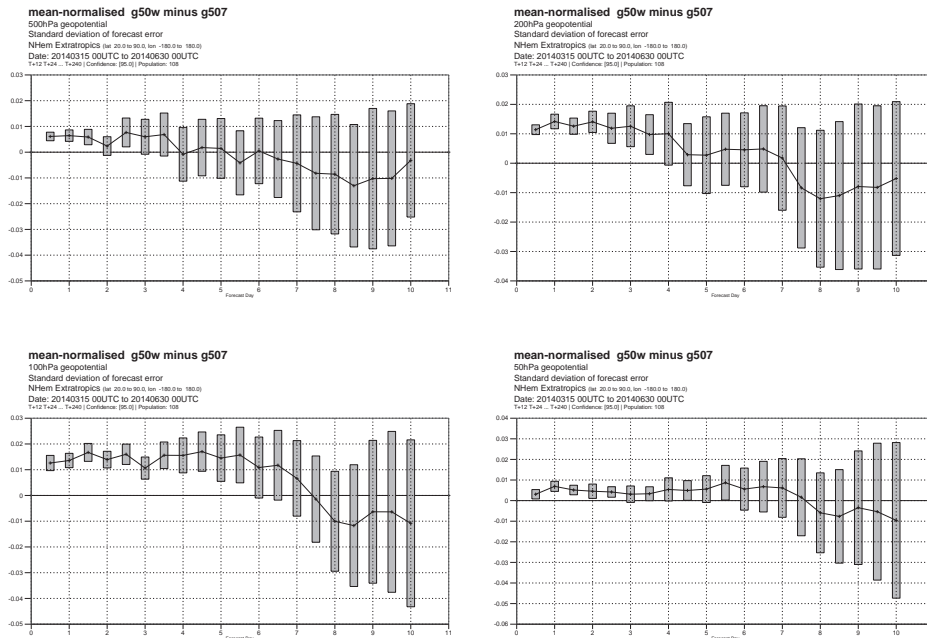


Figure 7: The fractional reduction in the standard deviation of geopotential height errors in the Northern Hemisphere at 500, 200, 100 and 50 hPa. Above the zero line indicates a positive impact and the error bars are the 95 % confidence intervals. The verification is against radiosondes.

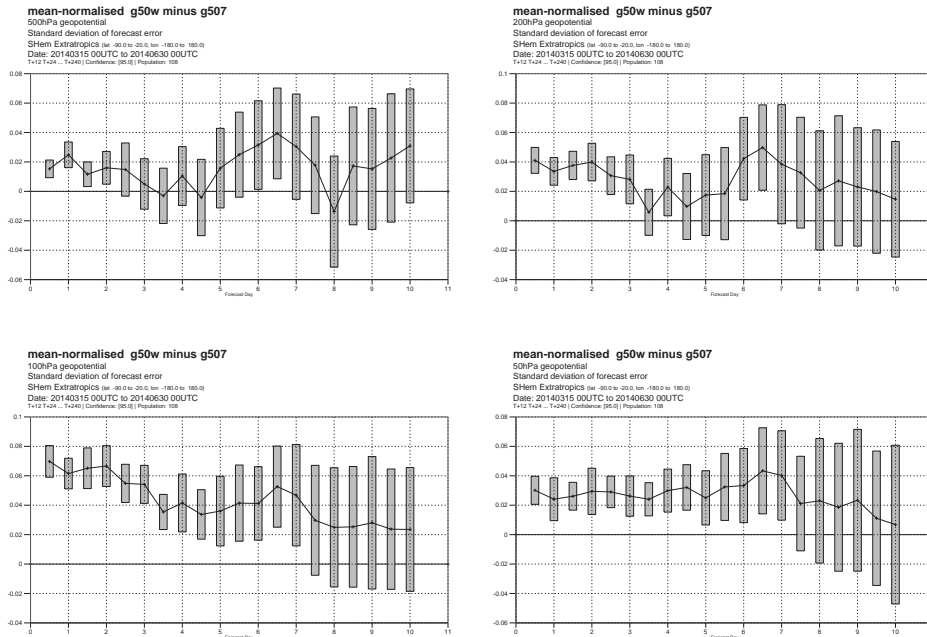


Figure 8: As Figure 7 but for the Southern Hemisphere.

4.2 Climate Applications

It seems reasonable to expect that climate monitoring applications of GPS-RO measurements will increase as the measurement time-series lengthens. GPS-RO measurements are now routinely assimilated into the ERA-Interim reanalysis (Poli *et al.*, 2010) producing a clear reduction in stratospheric temperature biases with respect to radiosondes since 2007, and producing better consistency between the ERA-Interim and the JRA-55 reanalyses in the lower/middle-stratosphere (Adrian Simmons personal communication.). The potential value of GPS-RO for climate monitoring is because the fundamental measurement is a time-delay with an atomic clock. It is argued that this can be measured more accurately than radiances, so GPS-RO measurements from different instruments should have the same bias/error characteristics, and they should be essentially interchangeable. Hence overlap periods for calibrating different GPS-RO instruments should not be required. The bending angle departure statistics produced with the ERA-Interim system can be used to test this hypothesis. Figure 9 shows the time-series of mean stratospheric bending angle (observed - forecast) departures for the GPS-RO data assimilated into ERA-Interim. The COSMIC measurements are assimilated from December 2006, and the Metop-A GRAS measurements are assimilated from May 2008. It is clear that the GRAS departures were initially biased by $\sim -0.2\%$ compared to the COSMIC. This difference was subsequently traced to the smoothing of the COSMIC excess phase delays, which was corrected in November 2009. This correction produced a clear convergence in the GRAS and COSMIC bias statistics, which is extremely encouraging. However, this does illustrate that we do not assimilate the raw GPS-RO measurements, and even pre-processing to the ionospheric corrected bending angles can introduce noticeable errors.

An important activity that also highlights the differences between the raw GPS-RO observations and the geophysical retrievals, in the climate monitoring context is the “RoTrends” project (e.g., Steiner *et al.*, 2013). In this project, the major international GPS-RO data centres process common datasets with their own version of the geophysical retrieval scheme outlined in section 2. The differences in monthly mean climatologies and trend values provide an estimate of the “structural uncertainty” in the GPS-RO retrievals. As expected, the best agreement between the centres is found at the bending angle level, providing some justification of the use of this variable in climate reanalyses.

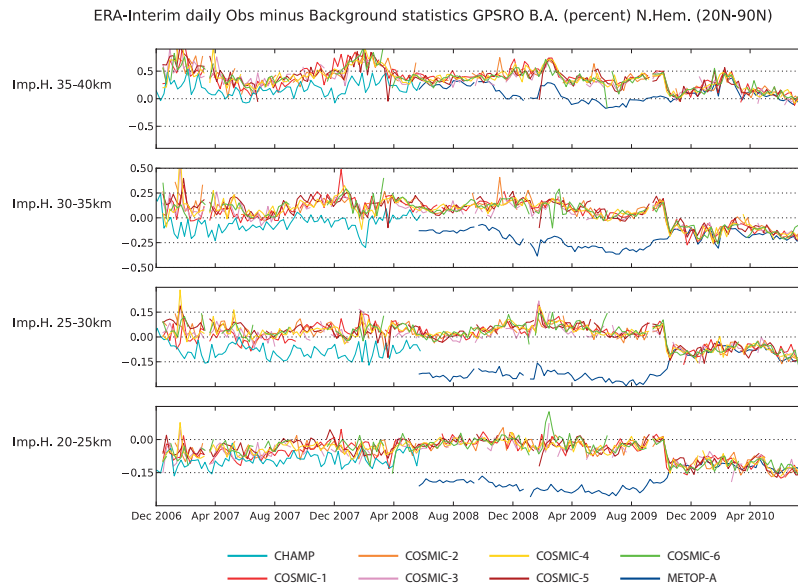


Figure 9: The time-series of GPS-RO bending angle departure statistics produced with the ERA-Interim reanalysis on four impact height intervals. A change was made to the COSMIC processing in November 2009 to correct the smoothing of the excess phase delays, producing a convergence of the COSMIC and Metop-A GRAS mean departure statistics.

5 Discussion

GPS-RO measurements are now a key component of the global observing system because they complement the information available from other observing systems. Their largest impact is in the stratosphere, reducing both random and systematic errors in short and medium-range forecasts. They are routinely used in climate reanalyses, and departure statistics produced with these systems show that the bending angle bias characteristics of different instruments are now very consistent in the stratosphere. However, it should still be recognised that GPS-RO measurements are not a direct measurement of atmospheric temperature, and that some temperature signals are difficult to detect with GPS-RO (e.g., Figure 3).

GPS-RO bending angles currently represent $\sim 3\text{-}4\%$ of the data assimilated in the ECMWF NWP system. A recent study by Harnisch *et al.*, (2013) suggests that there is a strong case for increasing the number of occultations per day from ~ 2500 to at least ~ 16000 . Improvements in the GPS-RO forward models and assumed error statistics should also increase the impact of this data in the future.

There are two areas where we might see increased use of GPS-RO observations in the coming years. The possibility of verifying NWP forecasts against GPS-RO bending angle measurements at the forecast time is currently being considered at ECMWF. It is likely to be most useful in the stratosphere, and it will provide much better sampling in the Southern Hemisphere than is available when verifying against radiosonde observations. The other area is testing global circulation models against monthly mean climatologies, derived from GPS-RO measurements. A preliminary study is underway at the Met Office, comparing the Hadley Centre model against monthly mean bending angle and refractivity climatologies produced by the ROM SAF. Clearly, the bias characteristics of the GPS-RO measurements are attractive in this context, but the advantage of this approach, rather than comparing the model against a climate reanalysis where GPS-RO has been assimilated, has to be investigated.

Acknowledgements

Sean Healy is a member of the Radio Occultation Meteorology Satellite Applications Facility (ROM SAF), which is a decentralised operational Radio Occultation processing centre under EUMETSAT. I would like to thank Tony McNally, Paul Poli, and Adrian Simmons their contribution to the work presented in this paper. Figure 5 was produced by Mohamed Dahoui. Figure 9 was produced by Paul Poli.

References

- Anthes, R. A., *et al.*, 2008: The COSMIC/FORMOSAT-3 Mission: Early Results. *Bull. Am. Meteorol. Soc.*, **89**, 313–333.
- Aparicio, J. M., and G. Deblonde, 2008: Impact of the assimilation of CHAMP refractivity profiles in Environment Canada global forecasts. *Mon. Wea. Rev.*, **136**, 257–275.
- Aparicio, J. M., and S. Laroche, 2011: An evaluation of the expression of the atmospheric refractivity for GPS signals. *J. Geophys. Res.*, **116**, doi:10.1029/2010JD015214.
- Bauer, P., G. Radnoti, S. Healy, and C. Cardinali, 2014: GNSS radio occultation constellation observing system experiments. *Mon. Wea. Rev.*, **142**, 555–572.
- Bean, B. R., and E. J. Dutton, 1968: *Radio Meteorology*. Dover Publications, New York.
- Burrows, C. P., S. B. Healy, and I. D. Culverwell, 2014: Improving the bias characteristics of the ROPP refractivity and bending angle operators. *Atmos. Meas. Tech. Discuss.*, **7**, 4439–4480.
- Cardinali, C., and S. Healy, 2014: Impact of GPS radio occultation measurements in the ECMWF system using adjoint-based diagnostics. *Q. J. R. Meteorol. Soc.*, **140**, 2315–2320. doi: 10.1002/qj.2300.
- Cucurull, L., and R. Anthes, 2014: Impact of infrared, microwave, and radio occultation satellite observations on operational numerical weather prediction. *Mon. Wea. Rev.*, **142**, 4164–4186.
- Cucurull, L., J. C. Derber, and R. J. Purser, 2013: A bending angle forward operator for global positioning system radio occultation measurements. *J. Geophys. Res.*, **118**, doi:10.1029/2012JD017782.
- Cucurull, L., J. C. Derber, R. Treadon, and R. J. Purser, 2007: Assimilation of Global Positioning System Radio Occultation Observations into NCEP's Global Data Assimilation System. *Mon. Wea. Rev.*, **135**, 3174–3193.
- Danzer, J., B. Scherllin-Pirscher, and U. Foelsche, 2013: Systematic residual ionospheric errors in radio occultation and a potential way to minimize them. *Atmos. Meas. Tech.*, **6**, 2169–2179.
- Eyre, J. R., 1994: Assimilation of radio occultation measurements into a numerical weather prediction system. Technical Memorandum 199, ECMWF, Reading, UK.
- Gorbunov, M., and K. Lauritsen, 2004: Analysis of wave fields by Fourier Integral Operators and their application for radio occultations. *Radio Sci.*, **39**, doi:10.1029/2003RS002971.
- Hajj, G. A., E. R. Kursinski, L. J. Romans, W. I. Bertiger, and S. S. Leroy, 2002: A technical description of atmospheric sounding by GPS occultation. *J. Atmos. Sol.-Terr. Phys.*, **64**, 451–469.
- Harnisch, F., S. B. Healy, P. Bauer, and S. J. English, 2013: Scaling of GNSS radio occultation impact with observation number using an ensemble of data assimilations. *Mon. Wea. Rev.*, **141**, 4395–4413.
- Healy, S. B., 2008: Forecast impact experiment with a constellation of GPS radio occultation receivers.

- Atmos. Sci. Lett.*, **9**, 111–118. DOI: 10.1002/asl.169.
- Healy, S. B., 2011: Refractivity coefficients used in the assimilation of GPS radio occultation measurements. *J. Geophys. Res.*, **116**, doi:10.1029/2010JD014013.
- Healy, S. B., 2013: Surface pressure information retrieved from GPS radio occultation measurements. *Q. J. R. Meteorol. Soc.*, **139**, 2108–2118. doi: 10.1002/qj.2090.
- Kursinski, E. R., G. A. Hajj, W. I. Bertiger, S. S. Leroy, T. K. Meehan, L. J. Romans, J. T. Schofield, D. J. McCleese, W. G. Melbourne, C. Thornton, T. P. Yunck, J. R. Eyre, and R. N. Nagatani, 1996: Initial results of radio occultation observations of earth's atmosphere using the Global Positioning System. *Science*, **271**, 1107–1110.
- Kursinski, E. R., G. A. Hajj, J. T. Schofield, R. P. Linfield, and K. R. Hardy, 1997: Observing earth's atmosphere with radio occultation measurements using the Global Positioning System. *J. Geophys. Res.*, **102**, 23.429–23.465.
- Luntama, J.-P., G. Kirchengast, M. Borsche, U. Foelsche, S. Steiner, S. Healy, A. von Engel, E. O'Clérigh, and C. Marquardt, 2008: Prospects of the EPS GRAS Mission for Operational Atmospheric Applications. *Bull. Am. Meteorol. Soc.*, **89**, 1863–1875.
- Poli, P., S. B. Healy, and D. P. Dee, 2010: Assimilation of Global Positioning System radio occultation data in the ECMWF ERA-interim reanalysis. *Q. J. R. Meteorol. Soc.*, **136**, 1972–1990. doi: 10.1002/qj.722.
- Poli, P., P. Moll, D. Puech, F. Rabier, and S. B. Healy, 2009: Quality control, error analysis, and impact assessment of FORMOSAT-3/COSMIC in numerical weather prediction. *Terr. Atmos. Ocean*, **20**, 101–113.
- Rennie, M. P., 2010: The impact of GPS radio occultation assimilation at the Met Office. *Q. J. R. Meteorol. Soc.*, **136**, 116–131. doi: 10.1002/qj.521.
- Rocken, C., R. Anthes, M. Exner, D. Hunt, S. Sokolovsky, R. Ware, M. Gorbunov, W. Schreiner, D. Feng, B. Herman, Y.-H. Kuo, and X. Zou, 1997: Analysis and validation of GPS/MET data in the neutral atmosphere. *J. Geophys. Res.*, **102**, 29.849–29.866.
- Rodgers, C. D., 2000: *Inverse methods for atmospheric sounding: Theory and practice*. World Scientific Publishing, Singapore, New Jersey, London, Hong Kong.
- Steiner, A. K., G. Kirchengast, and H. Ladreiter, 1999: Inversion, error analysis, and validation of GPS/MET occultation data. *Ann. Geophys.*, **17**, 122–138.
- Steiner, A. K. *et al.*, 2013: Quantification of structural uncertainty in climate data records from GPS radio occultation. *Atmos. Chem. Phys.*, **13**, 1469–1484.
- Vorob'ev, V., and T. Krasil'nikova, 1994: Estimation of the accuracy of the atmospheric refractive index recovery from doppler shift measurements at frequencies used in the NAVSTAR system. *USSR Phys. Atmos. Ocean, Engl. Transl.*, **29**, 602–609.
- Wickert, J., C. Reigber, G. Beyerle, R. König, C. Marquardt, T. Schmidt, L. Grunwaldt, R. Galas, T. Meehan, W. Melbourne, and K. Hocke, 2001: Atmosphere sounding by GPS radio occultation: First results from CHAMP. *Geophys. Res. Lett.*, **28**, 3263–3266.
- Yunck, T. P., C.-H. Liu, and R. Ware, 2000: A history of GPS sounding. *Terr. Atmos. Ocean*, **11**, 1–20.